APSEC 2015

INFLUENCE OF GREEN CORROSION INHIBITOR ON REINFORCED CONCRETE ATTACKED BY MAGNESIUM SULPHATE

Mohammad Ismail[1] & Asipita Salawu Abdulrahman[2]*

[1]*UTM Construction Research Centre, Faculty of Civil Engineering, Universiti Teknologi Malaysia*
[2]*Department of Materials and Metallurgical Engineering, Federal University of Technology, Minna, Nigeria,*

*Corresponding Author: *asipita.salawu@futminna.edu.ng*

Abstract. Sulphate attack is one of the phenomena that may cause gradual but severe damages to concrete structures durability. Sulphate attack is due to a series of chemical reactions between sulphate ions and principle components of the cement paste microstructure. In this work the effects of 1.5% and 4.5% $MgSO_4$ additions on concrete durability of 0.45 and 0.65 water/cement ratios (w/c) and the residual effects on corrosion of steel reinforcement were investigated using concrete resistivity. The results shows that 2% addition of *Bambusa arundinacea* green inhibitor improved the concrete resistivity of $MgSO_4$ contamination concrete by 54% and 64% for 0.45 and 0.65w/c ratios respectively. Thus comparatively, *Bambusa arundinacea* inhibitor performed far better than Calcium nitrite, Ethanolamine inhibitors and even the non-contaminated control sample. This confirmed a linear relationship between concrete resistivity and probability of corrosion in concrete. Concrete resistivity has proven to be effective parameter for the estimation of the risk of steel reinforcement in concrete.

Keywords: *Sulphate attack, concrete resistivity, green inhibitor, corrosion*

1.0 Introduction

Sulphate attack is one of the phenomena that may cause gradual but severe damages to concrete structures durability. Sulphate attack is due to a series of chemical reactions between sulphate ions and principle components of the cement paste microstructure. The United State Bureau of Reclamation warned that concentrations of soluble sulphate greater than 0.1% in soil may have deleterious effect on concrete and more than 0.5% soluble sulphate in soil may have serious effect (Irassar, 2009). Many degradation processes in cement-based materials include the diffusion of one or more chemical species into concrete and consequent chemical reactions, which alter the chemical and physical nature of the microstructure. External sulfate attack is mostly described by a

coupled diffusion–reaction mechanism that leads to the decomposition of hardened cement constituents and cracking of the paste (Abdulrahman *et al*., 2011).

Sulphate attack is one of the most aggressive environmental deteriorations that affect the long-term durability of concrete structures and can cause huge economic loss. For concrete in marine environment, drying–wetting cycles can accelerate the deterioration of concrete such as in the environment like splash and tidal zone. Furthermore, concrete in marine environment endures multifarious loading all the time. The concrete in the splash and tidal zone of marine environment suffers from the deterioration of the coupling function of salt solution, drying–wetting cycles and mechanical loading. There have been many reports on the damage process of concrete exposed to sulphate attack (Bassuoni and Nehdi, 2009; Bellmann *et al*., 2006) and the coupling function of sulphate attack and drying–wetting cycles. Sulphate attack is one of the main reasons that can cause coastal structures to fail. Having penetrated into concrete, sulphate ions can react with cement hydration products to form gypsum and ettringite; the latter is also called delayed ettringite. The nucleation and growth of ettringite may take place in the pores of concrete. If the pores are not large enough to accommodate the expansive products, internal expansive forces will be produced. Under the action of the expansive forces, tensile stresses will be generated at pore surfaces and the nucleation of micro-cracks may then occur (Brown *et al*., 2000; Brown and Steven, 2000). The evolution of micro-cracks will significantly accelerate the penetration of sulphate ions in concrete, and thus cause deterioration of the structures (Girardi and Di, 2011).

Consequently, in this work the effects of 1.5% and 4.5% $MgSO_4$ additions on concrete durability of 0.45 and 0.65 water/cement ratios (w/c) and the residual effects on corrosion of steel reinforcement were investigated. $MgSO_4$ salt was chosen as a result of being pronounced as more aggressive in groundwater than any other salt by Irassar, 2009. Inhibitors (*Bambusa Arundinacea*, Calcium nitrite and Ethanol amine) were added to the mix in order to ascertain their efficacies.

2.0 Materials and Methods

2.1 Materials

Laboratory specimens were cast to simulate reinforced concrete suffering from corrosion as a consequence of sulphate attack designed for 30MPa of 28 days compressive strength. This concrete was designed to provide favorable environment for corrosion of the steel reinforcement to occur. The laboratory concrete specimens were manufactured from Ordinary Portland Cement (OPC). It is part of the consignments (or direct order) to the Faculty of Civil Engineering, Universiti Teknologi Malaysia, Structure and Materials laboratory. However, care was always exercised to ensure freshness of all cements.

The powdered leaves were extracted using 95% ethanol. Two methods used were in accordance to Abdulrahman (2012).

Sulphate was mixed into the concrete as magnesium sulphate of analytical reagent grade. The concentrations of magnesium sulphate used were 1.5% and 4.5% by mass of cement and the corresponding sulphate concentrations were 1.2% and 3.6%, respectively. Maximum coarse aggregates of size 20 mm and 10 mm of quartzite origin were used in the ratio of 1.78:1 to satisfy the overall grading requirement of coarse aggregate (Pradhan and Bhattacarjee, 2009). Land quarried sand conforming to zone II classification of British standard BS 1881-125 and MS EN 12620 was used as fine aggregate. Tap water from laboratory of deep ground water source was used for the preparation of specimens. All the concrete mixes were designed for similar workability with slump of 30–60 mm. The water content was kept constant to 230 kg/m^3 for the desired slump in all the mixes to have similar workability. Two water–cement ratios (w/c) used were 0.45 and 0.65. The cement contents for different concrete mixes were calculated by dividing the water content by the corresponding w/c ratios. The fresh density of concrete was then obtained as per guidelines specified by British method of mix selection (DOE) to be 2380Kg/m^3. After that, the aggregate contents were calculated. The w/c ratio, cement content, water content, fine aggregate content and coarse aggregate content of the concrete mixes made of OPC is presented in Table 1.

Table 1: Concrete mix proportions

Water-cement Ratio (w/c)	Water content (kg/m^3)	Cement content (kg/m^3)	Fine aggregate Content (kg/m^3)	Coarse aggregate content (kg/m^3)
0.45	230	511	623	1016
0.65	230	354	754	1042

Steel bars were cut to the required length of 240 mm. With the mixes designs of 1:1.2:2 and 1:2.1:2.9 for water/cement ratios of 0.45 and 0.65 respectively, to simulate good and poor quality concrete, that was expected to offer only limited corrosion protection to steel at 25 mm cover depths. Each steel specimen was cleaned in acetone, polished very lightly with grade 1600 emery, washed in deionized water and dried with a lens tissue before being stored in a desiccators for several days prior to being used. They were insulated at the lower end and at the upper part with concrete to prevent crevice corrosion.

The specimens were demoulded after 24 h of casting, cured in seawater for 28 days and exposed for 360 days of wet and dry cycles (Saraswathy *et al*., 2001). The corrosion behaviours of embedded steel in concrete were monitored by Electrochemical Impedance Spectroscopy (EIS) and Linear Polarization Resistance (LPR) in accordance to the method used by Asipita *et al*. (2014). Corrosion rate by gravimetric (mass loss)

measurement and Field Emission Scanning Electron Microscopy (FESEM) were carried for structural morphology at the age of 1 year after completion of EIS and LPR tests.

3.0 Results and Discussion

3.1 Effects of $Mgso_4$ Additions on Concrete Strength of 0.45 Water/Cement Ratios

The results of the compressive strength test indicated that the additions of *Bambusa Arundinacea*, Calcium nitrite and Ethanolamine inhibitors increased the compressive strength of concrete when compared to the control sample. Meanwhile, 360 days compressive strength of *Bambusa arundinacea* is higher than the other two inhibitors (Calcium nitrite ($Ca(NO_2)_2$) and Ethanolamine (C_2H_7NO)) in Tables 2 and 3. This can be attributed to the presence of electronegative functional groups and π-electrons in their structures. It formed conjugated double bonds that prevent water permeability into the concrete to initiate sulphate attack.

Table 2: Compressive strength test (MPa) for 0.45 W/C ratios of 1.5% $MgSO_4$ additions

System	*Curing Duration*				
	7 days	*28 days*	*90 days*	*180 days*	*360 days*
Control	30.83	43.27	54.87	41.31	55.53
$MgSO_4$ attack	31.60	43.28	54.20	44.06	56.40
2% $Ca(NO_2)_2$ inhibitor	40.80	68.30	58.55	48.42	77.20
4% $Ca(NO_2)_2$ inhibitor	47.82	52.51	49.85	45.21	49.10
2% C_2H_7NO inhibitor	42.91	56.69	56.80	62.14	62.71
4% C_2H_7NO inhibitor	38.53	51.04	54.90	71.54	66.29
2% Green *Bambusa arundinacea* inhibitor	35.52	48.36	58.92	63.52	83.46
4% Green *Bambusa arundinacea* inhibitor	33.71	45.58	58.43	61.95	79.12

This bonds formed are hydrophobic as a result of heteroatom of quaternary nitrogen atom and aromatic ring which blocks concrete pores (Hekal *et al*., 2002; Ismail *et al*., 2010; Sideris *et al*., 2006). The water in contact with a porous hydrophilic concrete, penetrates the it by means of capillary forces following the Washburn equation, $p = (2\gamma/r_c)\cos\sigma$, where γ represents the liquid surface tension, r_c is the capillary pore radius, and σ is the contact angle. A water droplet, on a hydrophilic concrete, wets the surface by spreading itself and by absorption through the solid porosity. If the contact angle becomes is less than 90°, p becomes positive and the liquid fills the pore spontaneously according to Abdulrahman *et al*., (2011).

However, in this case Bambusa arundinacea hydrophobic agents lowered the molecular attraction between water and the concrete pore walls. Where the contact angle becomes higher than 90°, the water droplet keeps it spherical, and an external pressure p (in this case negative) is necessary to allow the liquid to penetrate the solid porosity. *Bambusa arundinacea* hinder liquid water to penetrate the structure when pressure is not excessively high. This is as a result of the pores containing high level of potassium and calcium from the inhibitor which combined with hydroxide to maintain the pH between 12 and 13. This high level of alkalinity passivates the steel, forming a dense gamma ferric oxide that is self-maintaining and prevent rapid corrosion.

Table 3: Compressive strength test (MPa) for 0.45 W/C ratios of 4.5% $MgSO_4$ additions

System	*Curing Duration*				
	7 days	*28 days*	*90 days*	*180 days*	*360 days*
Control	30.83	43.27	54.87	41.31	55.53
$MgSO_4$ attack	26.98	41.44	47.00	42.73	52.18
2% $Ca(NO_2)_2$ inhibitor	30.09	51.51	52.73	40.39	67.13
4% $Ca(NO_2)_2$ inhibitor	23.01	53.59	51.25	40.31	65.90
2% C_2H_7NO inhibitor	24.96	33.42	45.90	43.10	48.59
4% C_2H_7NO inhibitor	33.52	45.60	52.07	51.77	36.16
2% Green *Bambusa arundinacea* inhibitor	36.94	48.53	59.20	63.76	71.83
4% Green *Bambusa arundinacea* inhibitor	21.65	34.25	60.80	44.44	64.16

3.2 Effects of $Mgso_4$ Additions on Concrete Strength of 0.65 Water/Cement Ratio

Generally, the compressive strength of high water/cement ratio (w/c 0.65) is low. Boyd and Mindess (2004) recommended the use of a lower w/c ratio to be more effective even than the use of sulphate-resistant cement in offsetting the detrimental effects of sulphate attack on concrete as there was significant drop in strength associated with high w/c. This is evident in the results obtained for all the inhibitors in Tables 4 and 5. The strength of control sample not is affected by sulphate attack as is higher in strength than the sulphate attack and inhibited samples.

Table 4: Compressive strength test (MPa) for 0.65 W/C ratios of 1.5% $MgSO_4$ additions

System	*Curing Duration*				
	7 days	*28 days*	*90 days*	*180 days*	*360 days*
Control	30.50	43.02	48.85	41.15	52.68
$MgSO_4$ attack	20.59	34.90	37.83	36.84	37.87
2% $Ca(NO_2)_2$ inhibitor	26.50	38.37	39.62	43.60	44.19
4% $Ca(NO_2)_2$ inhibitor	19.80	31.23	35.00	35.77	38.38
2% C_2H_7NO inhibitor	18.17	33.73	39.85	45.05	42.00
4% C_2H_7NO inhibitor	17.51	31.61	36.28	40.39	44.17
2% Green *Bambusa arundinacea* inhibitor	19.09	28.81	31.91	44.07	41.97
4% Green *Bambusa arundinacea* inhibitor	18.19	27.55	30.86	41.43	39.81

Table 5: Compressive strength test (MPa) for 0.65 W/C ratios of 4.5% $MgSO_4$ additions

System	*Curing Duration*				
	7 days	*28 days*	*90 days*	*180 days*	*360 days*
Control	30.50	43.02	48.85	41.15	52.68
$MgSO_4$ attack	18.54	32.42	37.98	34.54	43.68
2% $Ca(NO_2)_2$ inhibitor	21.29	26.32	40.35	49.53	52.25
4% $Ca(NO_2)_2$ inhibitor	19.31	23.17	38.60	40.80	48.31
2% C_2H_7NO inhibitor	15.59	33.46	40.45	31.59	33.80
4% C_2H_7NO inhibitor	10.96	23.30	32.62	35.18	37.60
2% Green *Bambusa arundinacea* inhibitor	19.78	28.11	33.82	38.34	33.06
4% Green *Bambusa arundinacea* inhibitor	16.22	21.04	29.84	40.08	35.71

3.3 Concrete Resistivity (ρ)

Concrete resistivity (ρ) was used to determine the suitability of the developed green *Bambusa arundinacea* inhibitor and others (Calcium nitrite and Ethanolamine inhibitors) to check external magnesium sulphate attack that causes a gradual dissolution of Portlandite (CH) and decomposition of the C-S-H phase in concrete. Concrete resistivity has proven to be effective parameter for the estimation of the corrosion risk of steel reinforcement in concrete. The correlations of electrochemical parameters such as corrosion potential (E_{corr}) and current density (I_{corr}) together with concrete resistivity are used in this section to ascertain the effects of $MgSO_4$ and the veracity of the inhibitors on the concrete. As aforementioned in literatures in chapter two sections, $MgSO_4$ has no detrimental effects on steel reinforcement in concrete, but expansive effect on concrete structures itself. Concrete resistivity was determined according to the formula used by Polder, (2009).

$$\rho = R_{c(measured)} \times {}^{B}/_{L} \quad (1)$$

Where:
ρ is the concrete resistivity (KΩcm)
R_c is the concrete resistance (KΩ)
B is the area of the core face (cm^2)
L is the length of the core (cm).

The of results electrochemical parameters as determined by linear polarization resistance (LPR) method, using portable corrosion meter and calculated concrete resistivity can be found on Tables 7.5 -7.8 of previous work by Abdulrahman, (2012).

According to Morris *et al*., (2002) reinforcing steels in concrete are likely to achieve an active state of corrosion when ρ is lower than 10 KΩcm, and likely to present a passive behaviour when ρ is higher than 30 KΩcm. Therefore, the results show that the concrete resistivity's (ρ) are generally above the passive limit for corrosion threat for all the samples, except for the $MgSO_4$ contamination samples at lower ages of 180-270 days. The results reveal that *Bambusa arundinacea* inhibitor improved the concrete resistivity of $MgSO_4$ contamination concrete by 54%, 26%, 64% and 40% for 1.5% and 4.5% $MgSO_4$ additions to 0.45 and 0.65 w/c ratios respectively after 360 days' exposure. Comparatively, *Bambusa arundinacea* inhibitor performed far better than Calcium nitrite, Ethanolamine inhibitors and even the non-contaminated control sample. Therefore, this behaviour of *Bambusa arundinacea* inhibitor might be attributed to its hydrophobic property that binds the movements of ions in concrete which ensure durable and longer life cycle of concrete.

On the other hand, other electrochemical results in the Tables 7.5-7.8 of Abdulrahman, (2012) correlated with the concrete resistivity results. This is in line with the investigation by Polder, (2009) which confirmed a linear relationship between concrete resistivity and probability of corrosion in concrete. For instance corrosion potential (E_{corr}) results indicated that E_{corr} is greater than -0.35mV, SHE. According to ASTM C876-09, any measured potential of less than -0.35V indicates corrosion activity with 90% probability. Any measured potential of greater than -0.20 V signifies no corrosion activity with 90% probability. On the other hand, corrosion activity is uncertain, if measured potential is between the above two limits. Therefore, the measured potentials in this case were generally greater than -0.20V. This clearly indicate that no threat to corrosion at the present exposure periods.

3.4 Microstructural Studies

Scanning electron microscopy (SEM) and energy dispersive x-ray (EDX) were used to study the formation of reaction products and their compositions in $MgSO_4$ contaminated and inhibited samples after 360 days of exposure. The damage evolution of the concrete caused by sulphate attack can be approximately represented by the damage

function expressed in terms of the immersion time of the specimen in sulphate solution and the sulphate concentration in the specimen are shown in Figures 1-11.

Image in Figure 1, (the control sample) still maintains a dense clustered structure devoid of expansion. Conversely, Figure 2 shows early formation of ettringite (the white background) because of sulphate ions interaction with some compound of cement paste (usually according to Irassar (2009) monosulfoaluminates (AFm-phases), hydrogarnet phases, unhydrated alumina phases and portlandite (CH)) causes expansive ettringite. Cracks initiation can be seen at ITZ.

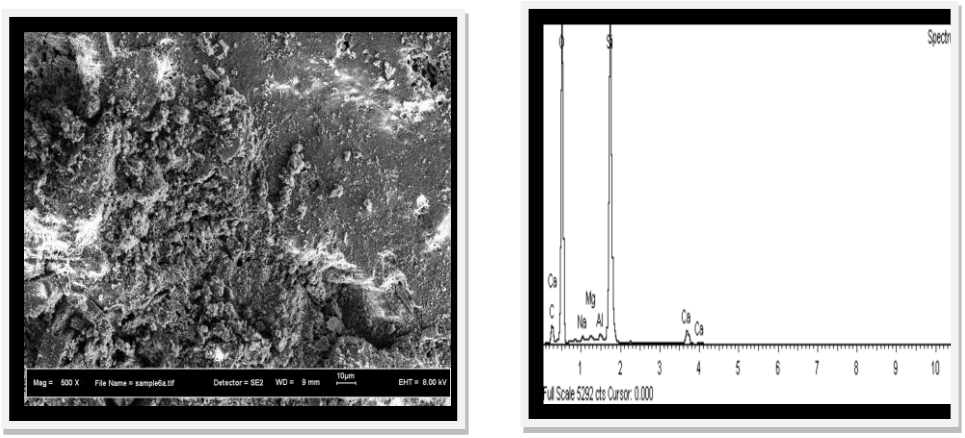

(a) **(b)**

Figure 1: Images of control sample (a) SEM and (b) EDX.

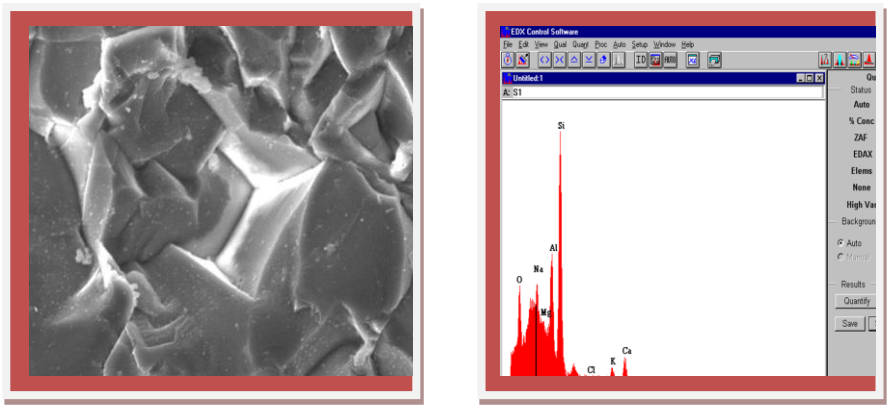

(a) **(b)**

Figure 2: Images of 1.5% $MgSO_4$ contamination to concrete (w/c 0.45), (a) SEM and (b) EDX.

The SEM/EDX images in Figures 3-4 for calcium nitrite and ethanol amine inhibited samples respectively, clearly reveals structures with portlandite ($Ca(OH)_2$) noticed at centre resulting in the formation of gypsum. The EDX shows high present of Mg^{2+}

which reacted with portlandite to form gypsum according to the following reaction reported by Brown and Steven, (2000).

$$MgSO_4 + Ca(OH)_2 \rightarrow CaSO_4.2H_2O + Mg(OH)_2 \quad (2)$$

The formation of this insoluble $Mg(OH)_2$ reduces the alkalinity of the concrete which releases more Ca^{2+} from C-S-H. Thus increasing the formation of gypsum and finally decomposes C-S-H to non-cementitious MSH. The aforementioned effect was also observed by Irassar, (2009) which he attributed to the complete depletion of $Ca(OH)_2$ due to magnesium attack that causes the provision of Ca^{2+} from C-S-H to solution, as observed in this case. Figure 5 shows *Bambusa arundinacea* inhibited sample which reveals a dense texture clustered formation of gypsum. In this case brucite ($Mg(OH)_2$) is not noticed as in the cases of calcium nitrite and ethanol amine inhibited samples.

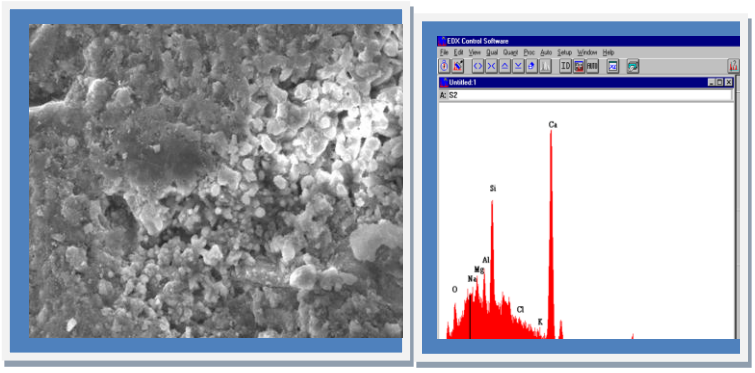

(a) (b)

Figure 3: Images of 2% $Ca(NO_2)_2$ inhibitor to 1.5% $MgSO_4$ contaminated concrete (w/c 0.45), (a) SEM and (b) EDX.

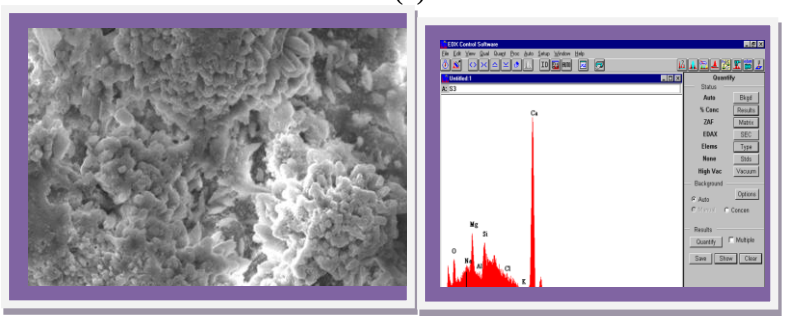

(a) (b)

Figure 4: Images of 2% C_2H_7NO inhibitor to 1.5% $MgSO_4$ contaminated concrete (w/c 0.45), (a) SEM and (b) EDX.

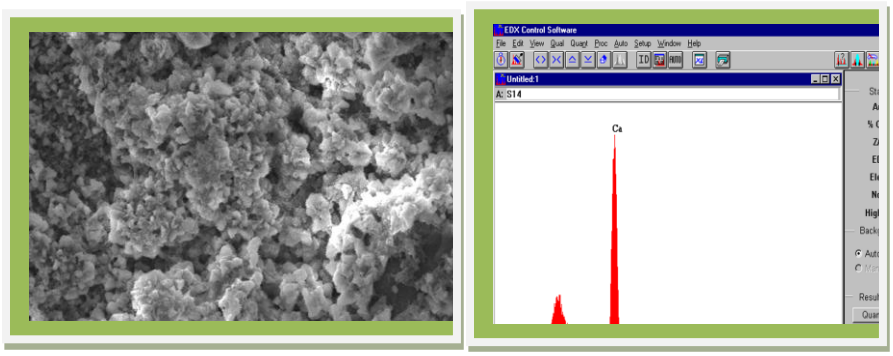

(a) (b)

Figure 5: Images of 2% Bambusa inhibitor to 1.5% $MgSO_4$ contaminated concrete (w/c 0.45), (a) SEM and (b) EDX.

Figure 6 reveals a deteriorated ettringite structure as a result of high amount of insoluble brucite that dissolved C-S-H. Due to the high $MgSO_4$ additions to the concrete, unstable cement phases (monocarboaluminates, monosulfoalumintes, hemicarboaluminates and hydrogarnets) transformed into ettringite. Decalcification of C-S-H was due to increase in C_3A hydrates resulting to the above unstable phases causing the cracks noticed in the structure. Chao *et al*., (2013) observed that both the cement hydration and the evolution of sulfate-induced damage have important influence on the penetration of sulphate ions in concrete. The evolution of sulfate-induced damage in concrete can significantly accelerate the penetration of sulfate ions, particularly when the sulfate concentration is high and/or the immersion time is longer.

Conversely, the structure in Figure 7 is a populated cluster of ettringite and Figure 8 showing cracks of disjointed clusters of ettringite forming prismatic crystals as a result of high w/c.

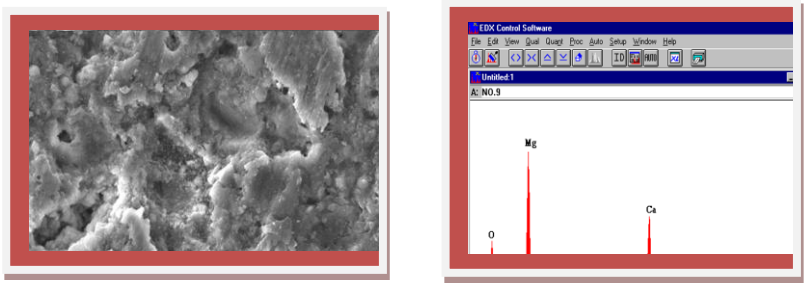

(a) (b)

Figure 6: Images of 4.5% $MgSO_4$ contamination to concrete (w/c 0.45), (a) SEM and (b) EDX.

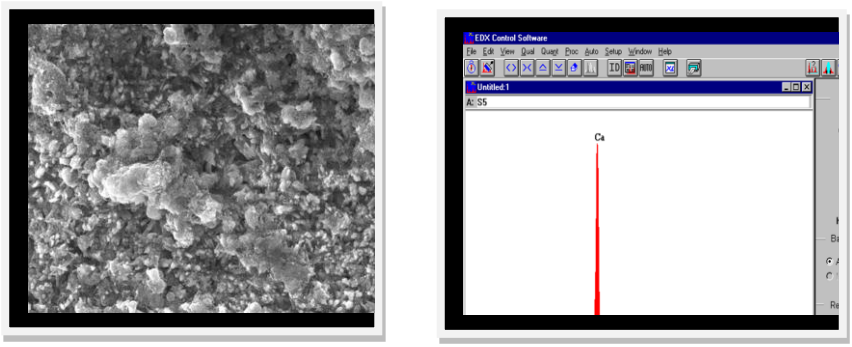

(a) (b)

Figure 7: Images of 1.5% $MgSO_4$ contamination to concrete (w/c 0.65), (a) SEM and (b) EDX.

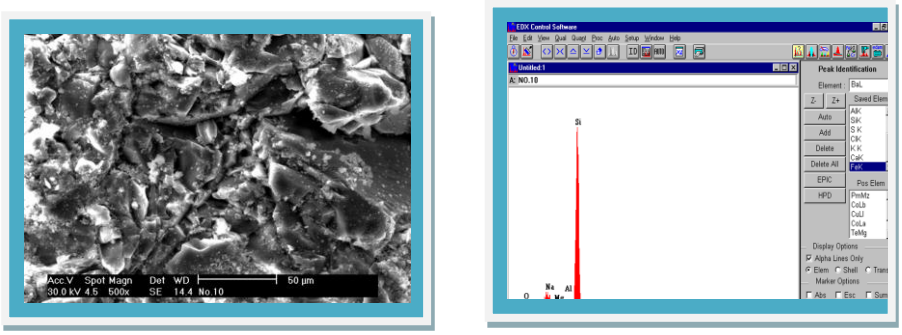

(a) (b)

Figure 8: Images of 4.5% $MgSO_4$ contamination to concrete (w/c 0.65), (a) SEM and (b) EDX.

Figures 9 show the formation of ettringite crystals that resulted to the cracks in the structure. Also in Figure 10, the structure is a mixture of ettringite and gypsum. The structures in both Figures indicated that these inhibitors (calcium nitrite and ethanol amine) cannot suppress magnesium sulphate ions in concrete. However, Figure 11 shows no traces of crack and ettringite formation. This might be attributed to high silicon content that buffers C-S-H phases, which probably converted virtually all the portlandite. This result confirms the high concrete resistivity of *Bambusa arundinacea* inhibitor already discussed above.

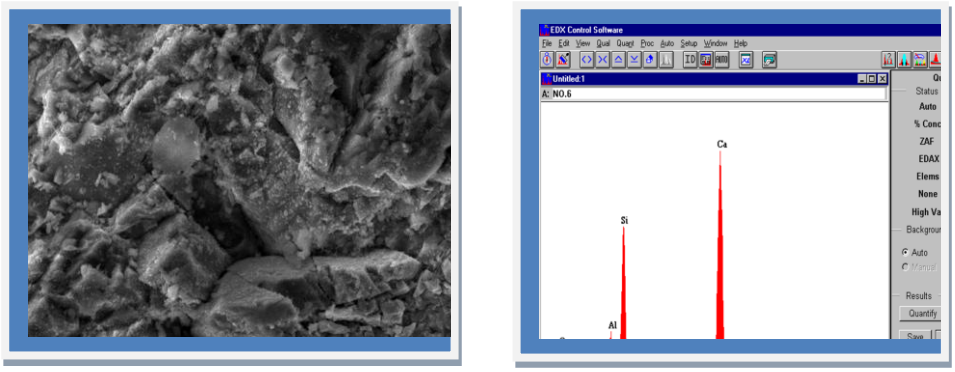

(a) (b)

Figure 9 Images of 2% $Ca(NO_2)_2$ inhibitor to 1.5% $MgSO_4$ contaminated concrete (w/c 0.65), (a) SEM and (b) EDX.

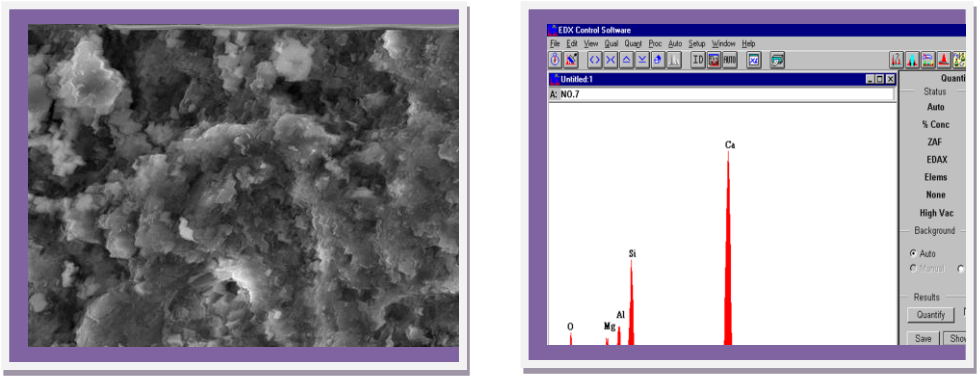

(a) (b)

Figure 10 Images of 2% C_2H_7NO inhibitor to 1.5% $MgSO_4$ contaminated concrete (w/c 0.65), (a) SEM and (b) EDX.

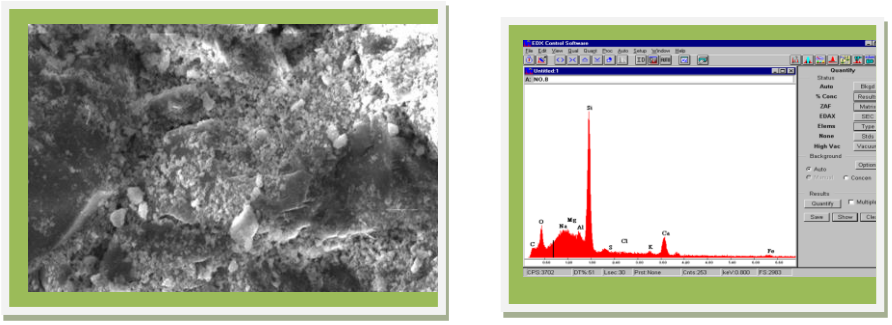

(a) (b)

Figure 11 Images of 2% Bambusa inhibitor to 1.5% $MgSO_4$ contaminated concrete (w/c 0.65), (a) SEM and (b) EDX.

4.0 Conclusions

Inhibitors additions to concrete attacked by sulphate increases the strength of the concrete. However, *Bambusa Arundinacea* was outstanding due its hydrophobic property that lowers the molecular attraction between water and the concrete pores. *Bambusa arundinacea* hinder liquid water to penetrate the structure when pressure is not excessively high. This is due to the pores containing high level of potassium and calcium from the inhibitor which combined with portlandite to maintain the pH of between 12 and 13. This high level of alkalinity passivates the steel, forming a dense gamma ferric oxide that is self-maintaining and prevent rapid corrosion.

The concrete resistivity's (ρ) were generally above the passive limit for corrosion threat for all the samples, except for the $MgSO_4$ contamination samples at lower ages of 180-270 days. Concrete resistivity has proven to be effective parameter for the estimation of the risk of steel reinforcement in concrete.

Bambusa arundinacea inhibitor improved the concrete resistivity of $MgSO_4$ contamination concrete by 54%, 26%, 64% and 40% for 1.5% and 4.5% MgSO4 additions to 0.45 and 0.65w/c ratios respectively. Thus, comparatively, *Bambusa arundinacea* inhibitor performed far better than Calcium nitrite, Ethanolamine inhibitors and even the non-contaminated control sample. This confirmed a linear relationship between concrete resistivity and probability of corrosion in concrete.

5.0 Acknowledgements

The authors acknowledge the research grants provided by Osaka Gas Foundation in Cultural Exchange (OGFICE) Research Grant Scheme and Universiti Malaysia Sarawak under Small Grant Scheme 02(S84)/820/2011(18). The authors would like to thank Bravo Green Sdn. Bhd. for providing the activated carbon.

References

Abdulrahman, A.S. (2012). *Performance of bambusa arundinacea as green inhibitor for corrosion of steel reinforcement in concrete*. PhD Thesis, Faculty of Civil Engineering, Universiti Teknologi Malaysia.

Abdulrahman A. S., Ismail M., and Hussain M. S. (2011). *Inhibiting Sulphate Attack in Concrete by Hydrophobic Green Plant Extract.* Advanced Materials Research Vols. 250-253, 3837-3843.

Asipita, S. A., Ismail, M., Abd Majid, M. Z., Abdul Majid, Z., (2014). *Green Bambusa Arundinacea leaves extract as a sustainable corrosion inhibitor in steel reinforcement concrete.* Journal of Cleaner production. Volume 67, page 139-146.

Bassuoni, M.T. and Nehdi, M. L. (2009). *Durability of self-consolidating concrete to sulfate*

attack under combined cyclic environments and flexural loading. Cement and Concrete Research 39(3): 206-226.

Bellmann, F., Möser, B. and Stark, J. (2006). *Influence of sulfate solution concentration on the formation of gypsum in sulfate resistance test specimen*. Cement and Concrete Research 36(2): 358-363.

Boyd, A.J. and Mindess, S. (2004). *The use of tension testing to investigate the effect of W/C ratio and cement type on the resistance of concrete to sulfate attack*. Cement and Concrete Research 34(3): 373-377.

British Standard. (1983). *BS 1881-125. Methods of mixing and sampling fresh concrete in the laboratory*. United Kingdom, BSI.

Brown, P., Steven, W.B. and Doerr, A. (2000). *Chemical changes in concrete due to the ingress of aggressive species*. Cement and Concrete Research 30(3): 411-418.

Brown, P. and Steven, W.B. (2000). *The distributions of bound sulfates and chlorides in concrete subjected to mixed NaCl, MgSO4, Na_2SO_4 attack*. Cement and Concrete Research 30(10): 1535-1542.

Chao Sun, Jiankang Chen, Jue Zhu, Minghua Zhang, Jian Ye (2013). *A new diffusion model of sulfate ions in concrete*. Construction and Building Materials 39 (2013) 39–45.

Girardi, F.M. and Di, R. (2011). *Resistance of concrete mixtures to cyclic sulfuric acid exposure and mixed sulfates: Effect of the type of aggregate*. Cement and Concrete Composites 33(2): 276-285.

Hekal, E. E., Kishar, E. and Mostafa, H. (2002). *Magnesium sulfate attack on hardened blended cement pastes under different circumstances*. Cement and Concrete Research 32(9): 1421-1427.

Irassar, E.F. (2009). *Sulfate attack on cementitious materials containing limestone filler -- A review*. Cement and Concrete Research 39(3): 241-254.

Ismail, M., Muhammad, B. and Ismail M.E. (2010). *Compressive strength loss and reinforcement degradations of reinforced concrete structure due to long-term exposure*. Construction and Building Materials 24(6): 898-902.

Malaysian Standard. (2010). *MS EN 12620. Aggregates for Concrete*. Cyberjaya, Department of Malaysian Standard.

Morris, W., Vico, A., Vázquez, M. and de-Sanchez, S.R. (2002). *Corrosion of reinforcing steel by means of concrete resistivity measurements*. Corrosion Science, 44: 81-99.

Polder, R.B. (2009). *Critical chloride content for reinforced concrete and its relationship to concrete resistivity*. Mater Corros. 60(8):623–30.

Pradhan, B. and Bhattacharjee B. (2009). *Performance evaluation of rebar in chloride contaminated concrete by corrosion rate*. Construction and Building Materials 23(6): 2346-2356.

Saraswathy V., Muralidharan, S., Kalyanasundaram, R.M., Thangavel, K. and Srinivasan, S (2001). *Evaluation of a composite corrosion-inhibiting admixture and its performance in concrete under macrocell corrosion conditions*. Cement and Concrete Research 31: 789-794.

Sideris, K.K., Savva, A.E. and Papayianni, J. (2006). *Sulfate resistance and carbonation of plain and blended cements*. Cement and Concrete Composites 28(1): 47-56.